Active Control of Thermoacoustic Amplification in a Thermo-Acousto-Electric Engine

Côme Olivier*, Guillaume Penelet, Gaëlle Poignand, Pierrick Lotton

Laboratoire d'Acoustique de l'Université du Maine UMR-CNRS 6613, Université du Maine, avenue Olivier Messiæn, 72085 LE MANS Cedex 9, France.
* Corresponding author: come.olivier@univ-lemans.fr

In this paper, a new approach is proposed to control the thermoacoustic amplification in a traveling-wave thermoacoustic engine. Based on the assumption that the spatial distribution of the self-established acoustic field in a stabilized regime does not necessary have the optimal shape for the most efficient thermal-to-acoustic conversion, this method uses an auxiliary acoustic source with a feedback loop applied on a thermo-acousto-electric transducer to improve its overall efficiency. After a brief presentation of the engine and its capabilities without any form of control, the preliminary results of an experimental study under various conditions are shown to demonstrate the possibility of a significant improvement in the thermoacoustic conversion with an appropriate tuning of the control parameters of the feedback loop. Applicability and further directions of investigation are also discussed.

1 Introduction

Short History of Thermoacoustics – The thermoacoustic effect has been known for a long time. Its most famous depiction is that of the sound emitted by the blowpipe of a glass-blower when heated by the molten glass at one end and kept at room temperature at the other end. It is regarded as a scientific curiosity until scientists achieve a recreation of the effect, like Byron Higgins [1] in the late 18th century who shows that it is possible to create an acoustic oscillation by applying appropriately a flame on a duct. In the following century, other experimental devices are designed by Sondhauss [2] – a tube with a closed heated end – and Rijke [3] – a heated wire mesh inserted in an open tube; both generate an acoustic wave thanks to a heat source. In parallel, Kirchhoff works on extending the theory of sound propagation; in 1868 he gives a first glimpse of the thermoacoustic interaction by introducing the effects of thermal conduction in gases. On this basis, the first qualitative explanation for thermoacoustic phenomena is given by Lord Rayleigh in 1896 [4], explaining the link between acoustic and temperature fields, and mostly the importance of the phase shift between the temperature variations of a particle in the neighborhood of the wall of a resonator subject to a strong temperature gradient and the particle acoustic velocity during an acoustic cycle.

From that moment, one has to wait until the 1960's for Carter to propose a great improvement to Sondhauss tube by introducing a stack of plates in the resonator to increase the global efficiency of the machine [5]. That is the first step leading to the standing-wave thermoacoustic machines, made of a waveguide, a stack of plates (or any other equivalent porous materials) and heat exchangers. A strong scientific interest is then taken in thermoacoustics, notably by Rott who establishes during the 70's and 80's the theoretical bases of the field [6], soon confirmed by the experimental work of Yazaki *et al.* [7] et

Wheatley [8]. With the team of Greg Swift in Los Alamos National Laboratory in the early 80's, research about thermoacoustics develops greatly.

About thermoacoustic machines – Thermoacoustic machines are part of the cyclic thermodynamic machines, based on the exchange of heat and work with their environment. They have two working modes: the *engine* mode, where the machine uses the transfer of heat from a hot source to a cold source to produce acoustical work; the *refrigerator* mode uses the acoustical power of an external source to produce a heat transfer from a cold source to hot one.

Many thermoacoustic engines (TAE) based on these principles have been developed with various geometries of resonators, leading one to rapidly distinguish two kinds of TAE : on one hand the engines wherein a quasi-standing wave develops, on the other hand those wherein the wave field is quasi-traveling, such engines often being called *Stirling engines*. This distinction is based on two criteria: on one hand, the phase relation between the oscillations of temperature and the particle acoustic velocity (corresponding either to a quasi-standing or a quasi-traveling wave); on the other hand, the kind of porous materials used as a thermoacoustic core a "stack" or a "regenerator". When a stack is used for standing wave engines, traveling wave TAE use a regenerator. The difference is in the nature of the contact of the fluid with the porous material : in a stack, the cycle is quasi-adiabatic and a particle follows a cycle close to Brayton cycle, whereas it is quasi-isotherm in a regenerator and a particle follows a quasi-ideal Stirling cycle. In terms of pore size, the pores of a stack have to be really larger than the thermal boundary layer thickness, the pores of a regenerator should be at most the same size.

In that last case, the ideal Stirling cycle of a particle nearby a wall presents a 90 degree-phase-shift between temperature and acoustic velocity. In the simplest description of its operation, this thermodynamic cycle may be divided in four periods: two phases of compression and relaxation (with temperature changes) and two phases of displacement at constant temperature and constant pressure. The idea of using the potentially high efficiency of that cycle is used by Ceperley to propose a traveling wave engine coupled to a refrigerator as soon as 1979 [9]. However, he is not able to build a working prototype by the time. It isn't before 1999 that Yazaki *et al.* [10] build the first traveling-wave thermoacoustic engine, followed a year later by Backhaus and Swift [11] with a high-power engine twice more efficient than the standing-wave engines built so far.

2 Experimental apparatus

The system used for this study is a prototype of thermo-acousto-electric transducer that has been designed in the Laboratoire d'Acoustique de l'Université du Maine, based on the work of Backhaus and Swift [12]. The experimental apparatus is composed of an annular thermoacoustic engine coupled to a ¼-wavelength resonator. The resonator contains an electrodynamic alternator, loaded by a closed cavity and whose role is to convert the produced acoustic power into electricity. A schematic view of this device is shown in Fig. 1.

This apparatus has been designed with the help of two different models: the free software DeltaEC developed at the Los Alamos National Laboratory [13, 14], and an internally developed model giving a linear description of the thermoacoustic amplification taking place in the annular resonator by mean of a depiction by transfer matrices [15]. The joint use of both models allows to come up with a thermoacoustic engine working with air at a low pressure (typically 5 bar) and with a reasonable onset temperature ($\Delta T < 300$ K when the alternator is loaded by an infinite resistance). Its onset frequency corresponds to the resonance frequency of the complete system, but is mostly governed by the ¼-wavelength resonator so that $f_{onset} \simeq 40$ Hz.

Description – In Fig. 1, one can notice that the torus-shaped section contains a larger-radius part comprising the temperature-inhomogeneous region of the engine. That section will later on be designated as the thermoacoustic core (TAC). It is represented in a more detailed fashion in Fig. 2.

The central piece of the TAC is the regenerator. It consists of a 2.3 cm-long stack of stainless-steel wire-mesh grids. The wires diameter is of 32 µm. The porosity of the regenerator is evaluated to $\varphi \simeq 0.69$ and its hydraulic radius is $r_h \simeq 20\,\mu$m.

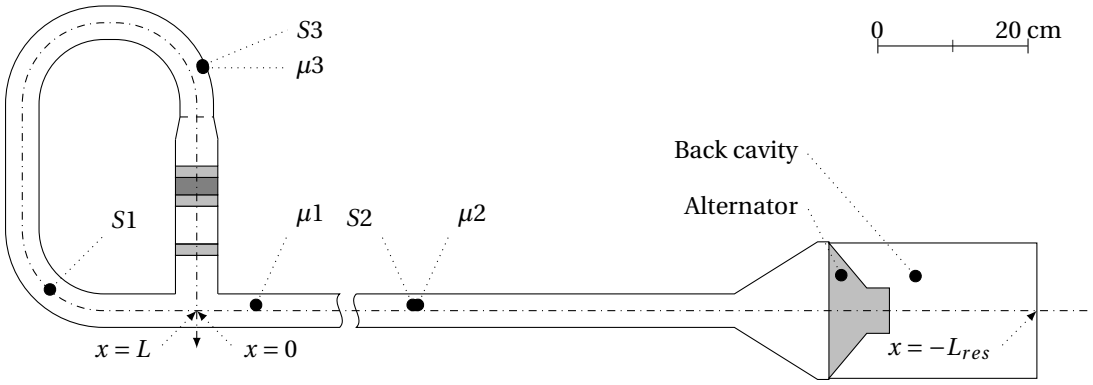

Figure 1: Scale schematic of the thermo-acousto-electric transducer being used for this study, designed at the Laboratoire d'Acoustique de l'Université du Maine.

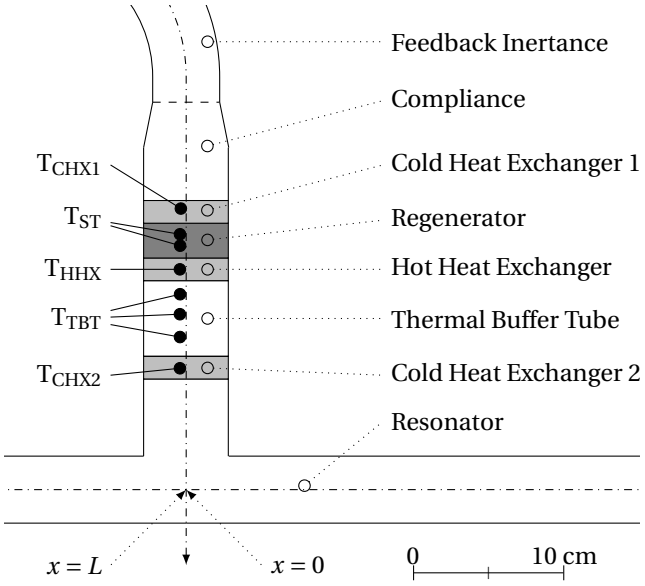

Figure 2: Scale schematic of the thermoacoustic core, showing the position of the temperature sensors.

At the top of the core is placed a first ambient heat exchanger. Made of a 15 mm-thick copper block drilled with 303 straight 2.0 mm-diameter holes. Its porosity is evaluated to $\varphi_{chx} \simeq 0.6$ (*cf.* Fig. 3). It is cooled by room-temperature water pumped from a tank and circulating in a circumferential groove through the shell at a rate of approximately $2 \times 10^{-4} \mathrm{m}^3/\mathrm{s}$.

The temperature gradient is imposed by a hot heat exchanger, just under the regenerator, which consists of a 2.0 m-long and 3.0 mm-wide nichrome ribbon inserted into a ceramic 0.9 mm-wide square-pores stack to form two perpendicular zigzags patterns covering a maximum of the section of the tube, as shown in Fig. 4. This exchanger is 15 mm-long and its estimated porosity is $\varphi_{hhx} \simeq 0.89$. It is driven by a high-power DC-power supply. An input heat power up to $\dot{Q}_h$ =180 W is provided through the hot heat exchanger, leading to a gas temperature up to 600 °C.Both the hot heat exchanger and the regenerator are inserted into a tube of ceramic to thermally insulate them from the shell and reduce the thermal leaks to the outside. The last element of the TAC, called the thermal buffer tube (TBT), is a 5 cm-long constant diameter open tube which provides a thermal buffer between the hot exchanger and the room temperature. It ends on a second cold heat exchanger that is in every respects similar to the first one.

The resonator is a straight 1.55 m-long, 42.15 mm-diameter tube that leads to a 121 mm-long cone to

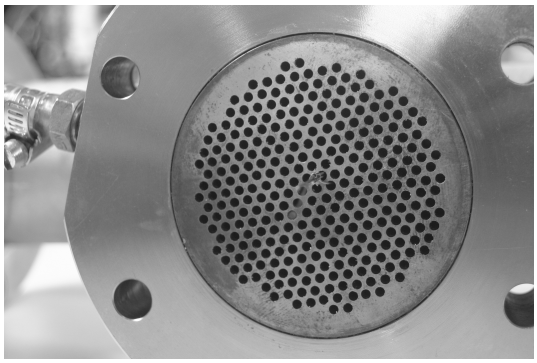

Figure 3: Cold heat exchanger with a room temperature water income on the left.

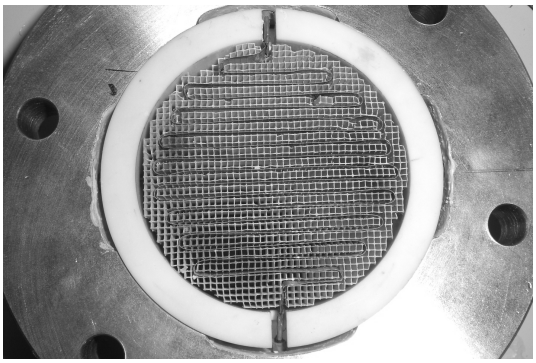

Figure 4: Hot heat exchanger inserted in the insulating ceramic ring.

adapt to the area of the electrodynamic loudspeaker – a Monacor SPH-170C – used as an alternator. The loudspeaker has been chosen for its low resonance frequency (38 Hz), close to that of the engine (40 Hz), and for its high force factor ($Bl = 8.95\,\mathrm{T\,m^{-1}}$). The back cavity is a 165 mm-long with a 91 mm-radius volume that acts as an acoustic compliance applied on the alternator in order to match its impedance to that of the rest of the engine.

Instrumentation – Eight 0.5 mm-diameter type-K thermocouples allow the measurement of temperatures throughout the core of the Stirling engine. Their placement in the middle of the three heat exchangers ($T_{\mathrm{CHX}(1,2)}$ and T_{HHX}), in the regenerator (T_{ST}) and along the TBT ($T_{\mathrm{TBT}(1,2,3)}$) is intended to measure the temperature profile in the core at any moment. Their position may be observed more precisely in Fig. 2.

Acoustic pressure is measured in three different points thanks to three high-resolution 5.54 mm-diameter pressure sensors located just on top of the thermoacoustic core ($\mu 3$) and in two different points of the resonator ($\mu 1$ and $\mu 2$), as can be seen in Fig. 1. The first one is used to evaluate the drive ratio DR

$$DR = \frac{p_3}{p_0}, \tag{1}$$

where p_3 is the amplitude of the pressure measured in the engine by microphone $\mu 3$ and p_0 is the value of the static pressure in the engine. The microphones on the resonator are used to evaluate the average available acoustic power in the resonator $\dot{W}_{res}$ as follows [16]:

$$\dot{W}_{res} = \frac{\pi r_0^2}{2\omega\rho\Delta x}\left[\left(1-\frac{\delta_\nu}{r_0}\right)|p_1||p_2|\sin\phi + \frac{\delta\nu}{2r_0}\left(|p_1|^2-|p_2|^2\right)\right], \tag{2}$$

with ρ the density of the working fluid, r_0 the inner-radius of the resonator, Δx the distance between the two microphones, ϕ the phase-shift between the signals p_1 and p_2 they measure and δ_ν the viscous boundary layer thickness at working angular frequency ω.

In order to evaluate the electrical power $\dot{W}_{el}$ generated by the alternator, it is connected to a variable electric load R_L across which the voltage U_L is measured, simply giving:

$$\dot{W}_{el} = \frac{U_{L,\mathrm{RMS}}^2}{R_L}. \tag{3}$$

Passive Improvements – The description of the working point of a thermoacoustic engine remains today given mostly by Rott's linear theory [6]. However, beyond the onset threshold, sound waves reach very large amplitudes and steady-state conditions (in terms of wave amplitude and temperature distribution) cannot be described by linear theory. Such effects as cascade of higher harmonics generation, (nonlinear) *acoustic streaming* (understand a mean fluid flow caused by acoustics), minor losses due

to sudden changes in section at the end of porous elements, etc., are to be taken into account to express the saturation of amplitude growth. All these phenomena highly reduce the overall efficiency of the engine by disturbing the temperature field and therefore the thermoacoustic amplification process.

Many techniques have been developed in order to counteract the nonlinear effects. Most of them consist in passive elements to be added to the engine at strategic locations. Here are some commonly applied solutions [17, 18]:

- tapered tubes: by giving a conical shape to the thermal buffer tube (TBT), the boundary-layer driven streaming – also called Rayleigh streaming – is minimized;
- flow straighteners: a short stack of wire-mesh screens ensures that the flow entering the TBT at the junction is spatially uniform and not a jet flow due either to the heat exchanger or the flow separation;
- jet pumps or membranes: a time-average pressure drop induced by converging nozzles allows to balance the Gedeon streaming due to the presence of a traveling wave.

Though they have been proven helpful in high power engines, intentionally none of these devices has been adapted to the present engine; this "control-free" situation allows to explore the possibilities for active control to improve global efficiency on all levels.

Active control apparatus – Passive elements, by the nature itself of their action – i.e. counteracting undesired non linear side-effects – are limited improvements. Their action consists in trying to bring back the operating mode of the engine to a linear regime, which is the ideal working point with a linear description.

Contrariwise, instead of curing the symptoms, the aim of active control (active in the meaning that there is an additional energy input) is to improve the overall efficiency by modifying the acoustical field so that the ideal operating point allows a higher efficiency. Indeed, the self-established acoustic field due to the thermoacoustic instability is highly bounded to the temperature field and interacts with it. The modification of the acoustic field by one or several auxiliary sources generates a disturbance in the temperature field in the thermoacoustic core which, in return, changes the thermoacoustic amplification. Several possibilities are then to be considered. The effect of a single auxiliary source driven by a feedback loop has to be explored. With two sources, it has been demonstrated [19] that it is possible to improve the overall efficiency of an annular engine by an appropriate tuning in phase and amplitude. However, the phenomena taking place in a more complex engine such as the thermo-acousto-electric transducer might differ from the simpler annular configuration. The focus will be here put on the opportunities offered by a single auxiliary source driven by a feedback loop, as shown in Fig. 5.

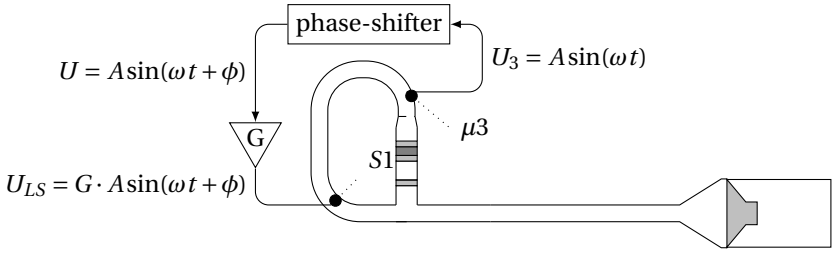

Figure 5: Schematic of the system with its single auxiliary-source active control system by a feedback loop.

The auxiliary source is a small mid-range low-power (5 W) speaker – a Visaton FRS 5 – loaded by a very small enclosure (only a few cm^3 on each side of the membrane). It is connected to the engine through a 27 mm-long capillary duct 6.5 mm in diameter. The small diameter of that connection allows to keep the coupling of the engine with the source to a minimum, in order not to change too much the characteristics of the engine. The source may be positioned at either of the three points noted $S1$ to

*S*3 on the schematic given in Fig. 1. It is powered by a feed-back loop, using the signal sensed by one of the three microphones and phase-shifted before to be amplified. The phase-shifter is a homemade device with three RC-shifter in series, allowing each a 135° shift. Voltage and current running through the speaker are monitored to gauge the supplied power for active-control $\dot{W}_{LS}$. The use of a feedback loop is interesting in this case, notably because it prevents the loss of synchronization between the thermoacoustic source and the auxiliary source [20], as the working frequency is likely to evolve with the temperature variations in the TAC.

Efficiency criteria – To evaluate the effects of the active control several criteria of efficiency are established. First of all is the overall efficiency η_{tot}, the one that is to be improved by the use of active control and defined as the ratio of the output power to the sum of the input powers:

$$\eta_{tot} = \frac{\dot{W}_{el}}{\dot{Q}_h + \dot{W}_{LS}}. \tag{4}$$

To insure that the active control affects the thermoacoustic conversion, the thermoacoustic conversion efficiency of the regenerator η_{reg} and acousto-electric conversion efficiency of the alternator η_{alt} are both monitored by the following approximations:

$$\eta_{reg} = \frac{\dot{W}_{res}}{\dot{Q}_h + \dot{W}_{LS}} \qquad \text{and} \qquad \eta_{alt} = \frac{\dot{W}_{el}}{\dot{W}_{res}}. \tag{5}$$

All measurements show that this last efficiency is very steady for the imposed working conditions. It changes slightly with the drive ratio from 40% to 42% when the input heat power goes from 70 to 150 W, but its variations for a series of measurement are under 1% and therefore negligible compared to that of η_{reg}. The results presented here will then be for η_{tot}, which is directly proportional to η_{reg}.

3 Experimental study of the performances of the thermo-acousto-electric transducer enhanced with single-source active control

In this section, to begin with, the performances of the engine without active control are exposed for later comparison. The effects of three control parameters of the active control are then studied, allowing three different series of measurements:

- for a fixed gain G of the audio power amplifier driving the auxiliary source, the effect of the phase-shift ϕ for various input heat powers $\dot{Q}_h$;
- for a fixed input heat power $\dot{Q}_h$, the effect of the phase-shift ϕ for various gain G;
- for a fixed appropriately chosen phase-shift ϕ_{opt}, the effect of the gain G for various input heat powers Q_h.

3.1 Preliminary qualification of the onset conditions and efficiency modifications due to the presence of the auxiliary source

When the auxiliary source is connected to the resonator, the behavior of the engine is modified due to the weak but existent coupling between the source and the engine. So the capabilities of the engine presented above (§2) are briefly evaluated, without any auxiliary source and when the auxiliary source is connected to the resonator. For this part of the study, the auxiliary source is not powered, but, in order to remain close to the operating conditions of active control, it is loaded with its complete powering chain switched on with the gain at zero. Mostly, this study consists in comparing the onset thresholds for the thermoacoustic instability, in terms of temperature gradient through the regenerator, for a load R_{load} at the alternator terminals that gives the highest global efficiency, as well as the amplitude growth

saturation under various heating conditions. The thresholds are determined using the following protocol: (1) the hot heat exchanger is brought to a balanced state of temperature known to be close but inferior to the threshold temperature (this first step take about 45 min); (2) the driving voltage of the heat exchange (i.e. the hot temperature) is increased by small steps; (3) a stabilization period necessary for the engine to reach thermal equilibrium is waited (a few minutes); (4) if no spontaneous oscillation appears, the heating power is further incremented.

The stationary behavior is also studied, by measuring the temperature difference between hot and cold heat exchanger ΔT, the global efficiency η_{tot}, and the drive ratio DR for different input heat powers. These results are presented along with the threshold conditions in Table 1. It is worth recalling here that the apparatus used for that experimental campaign has not been designed as an industrial prototype but as a "proof-of-concept" model, used for experimental validation of analytic and numeric models. Working with air at low pressure, its maximum efficiency is about 1%.

Table 1: Onset and saturation conditions of the TAE before ($\varnothing$) and after addition of the active control apparatus (not powered) at position $S1$. Efficiency η_{tot} and drive ratio DR are given in [%].

	Onset conditions			Saturation conditions					
				$Q_h = 70W$			$Q_h = 140\,\mathrm{W}$		
aux. source	f_o [Hz]	ΔT_o [K]	$Q_{h,o}$ [W]	ΔT [K]	η_{tot}	DR	ΔT [K]	η_{tot}	DR
$\varnothing$	40.88	374.5	57.8	367	0.25	0.71	411	0.71	3.16
S1	40.18	419	69.8	400	0.14	0.59	456	0.60	2.75

All results presented further are in the form of an efficiency normalized by the efficiency when the amplification gain is $G = 0$. The gain G of the feedback loop is defined for everything that follows as the ratio of the tension U_{LS} driving the active control speaker over the tension U_3 delivered by the pressure sensor at position $\mu 3$:

$$G = \frac{U_3}{U_{LS}}. \tag{6}$$

3.2 Effect of phase-shift ϕ for a given gain G

A first interest is taken in the influence of the phase-shift between the measured signal at position $\mu 3$ and the voltage of the signal driving the source at position $S1$, for a given amplification gain $G = 1$ or $G = 3.2$ and for different heat inputs. The results are presented in Figs. 6 and 7.

With the phase-shift varying, two domains are to be distinguished: one where the efficiency is improved (roughly from 180 to 360°) up to more than 25% in the case presented here (that number going as high as 80% with $G = 10$ for $Q_h = 70\,\mathrm{W}$, see Fig. 8 or 11), and one where the efficiency is decreased (from 0 to 180°). The improvement or deterioration of performances brought by the active control is greater for low drive ratios (DR), as the working point is closer to the onset condition. Since the active control power $\dot{W}_{LS}$ is proportional to the acoustic power $\dot{W}_{loop}$ in front of the reference microphone, the effect of the active control for a constant gain does not have a constant amplitude. Moreover, in the unfavorable domain, there exist conditions bringing to the death of the self-sustained oscillations – phenomenon known as *quenching*. The lower the DR is, the larger the domain of quenching seems to be for of given gain. Both behaviors described here are indicative of nonlinear interaction between the autonomous thermoacoustic oscillator and the loudspeaker.

3.3 Effect of phase-shift ϕ for a given input heat power $\dot{Q}_h$

The focus is now brought on the influence of the phase-shift between the measured signal at position $\mu 3$ and the voltage driving the source at position $S1$, for a given input heat power $\dot{Q}_h = 70\,\mathrm{W}$ and for different values of gain of the amplification in the feedback loop. The results are presented in Fig. 8. In Figure 9 are presented the variations of the corresponding temperature gradient $\Delta T = T_{\mathrm{HHX}} - T_{\mathrm{CHX1}}$.

In the zone of unfavorable phase-shift, the gain may be incremented to reach a value for which the engine quenches at a single value of phase-shift $\phi \simeq 90°$ (here, that gain value is $G \simeq 3$). With the aug-

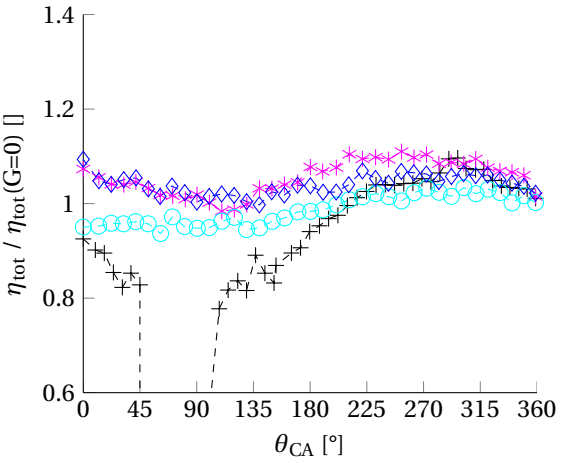

Figure 6: Evolution of the normalized efficiency with the variation of the phase-shift for a heat supply $\dot{Q}_h$ = 70 W (+), 80 W (*), 90 W (o) or 100 W (◇) and a constant gain $G = 1$.

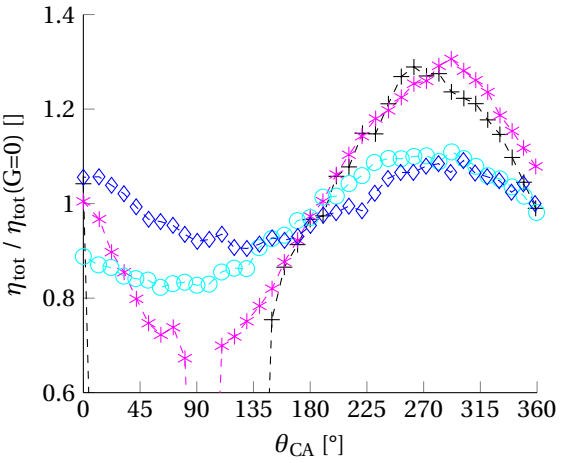

Figure 7: Evolution of the normalized efficiency with the variation of the phase-shift for a heat supply $\dot{Q}_h$ = 69.9 W (+), 70.5 W (*), 80 W (o) or 110 W (◇) and a constant gain $G = 3.2$.

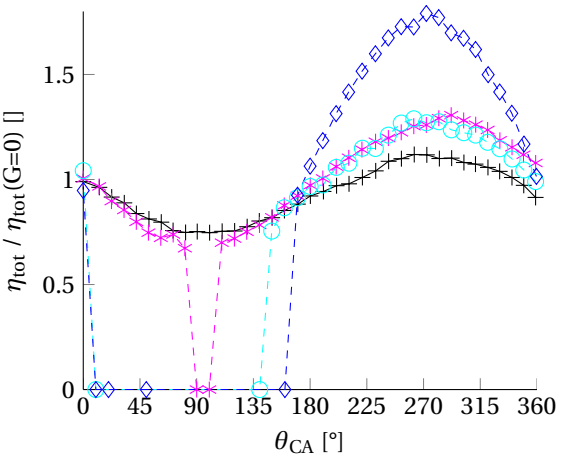

Figure 8: Evolution of the normalized efficiency for a given heat supply of 70 W and several values of gain: G = 2.0 (+), G = 3.0 (*), $G = 3.2$ (o) or $G = 10$ (◇).

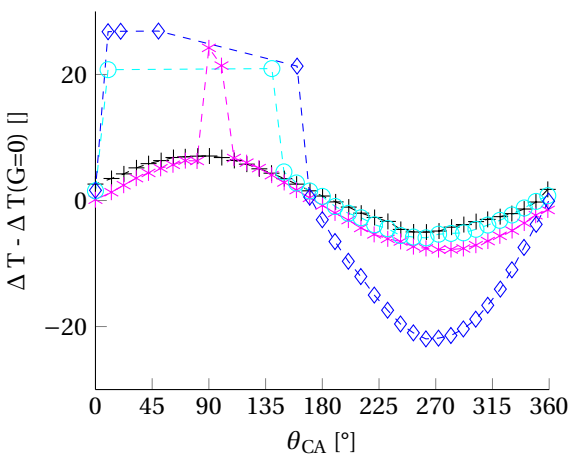

Figure 9: Evolution of the temperature gradient for a given heat supply of 70 W and several values of gain: G = 2.0 (+), G = 3.0 (*), $G = 3.2$ (o) or $G = 10$ (◇).

mentation of the gain, the domain of quenching enlarges rapidly, until it concerns the complete domain between 0 and 180° for the largest values of gain. As the engine quenches, the temperature difference raises then to a stable level, namely the temperature reached in absence of thermoacoustic oscillation.

In the domain of favorable phase-shifts, the efficiency of the TAE is increased as the gain of amplification in the feedback loop raises. In parallel, the temperature difference ΔT between hot and cold heat exchangers shows a significant decrease (up to 25°) combined with the increase of efficiency as can be seen in Fig. 9. This confirms the hypothesis emitted at the beginning: there exists a more favorable acoustic field for thermoacoustic conversion than the self-established field, for which more thermal energy is converted to acoustic power.

3.4 Effect of the gain G for an optimal phase-shift ϕ_{opt}

Finally, choosing a phase-shift $\phi \simeq 270°$ hat seems to be optimal for various heat inputs, the influence of a variation of the gain G of the amplification of the feedback loop is observed. Experimental evolution of output electric power is shown in Fig. 10 and evolution of the efficiency of thermoacoustic conversion in Fig. 11.

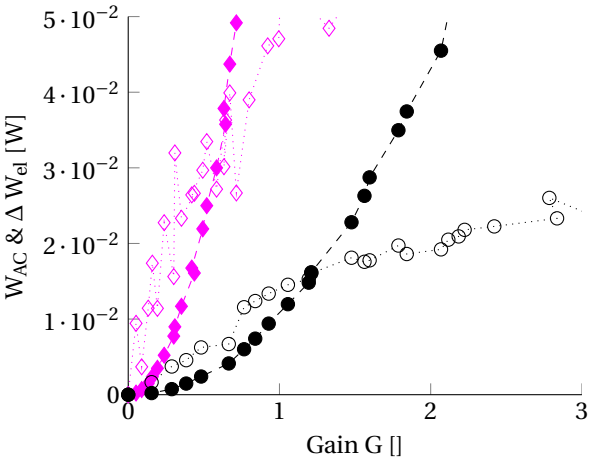

Figure 10: Evolution of the extra electrical power produced (···) with the variation of the power supplied to the auxiliary source (- -), for a given heat supply of 70 W (o) or 140 W (◇) and a constant 90°-phase-shift.

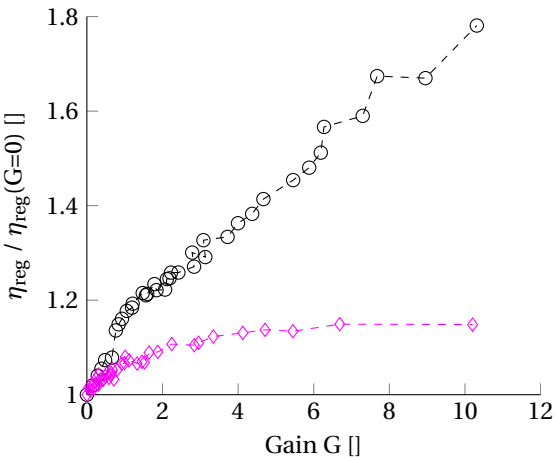

Figure 11: Evolution of the efficiency with the variation of the power supplied to the auxiliary source, for a given heat supply of 70 W (o) or 140 W (◇) and a constant 90°-phase-shift.

In order that the active control is undoubtedly a profitable operation, the extra power produced thanks to the active control has to be larger than the power injected into the active control device. A zone clearly exists in both cases, until $G \simeq 1.2$ for $\dot{Q}_h = 70\,\text{W}$ and $G \simeq 0.7$ for $\dot{Q}_h = 140\,\text{W}$ where the output power increase is greater than the power driving the active control.

When the DR is increased, that is when the heating power is increased, the active control added power required to observe a significant improvement of the efficiency raises faster than the extra power produced. The sum of the input powers $\dot{Q}_h + \dot{W}_{LS}$ then grows faster than the output power $\dot{W}_{el}$, leading to a *saturation* in the augmentation of the efficiency, as seen for the configuration of highest DR in Fig. 11. The behavior described here is one more time indicative of nonlinear interaction taking place in the active control process.

4 Discussion and conclusion

From the experimental study presented in the previous section (§3), it appears that the use of a single source active control apparatus to improve the efficiency of thermoacoustic amplification in a thermoacoustic engine is a promising technical solution. Bringing to light various phenomena as *quenching* and *saturation*, it clearly involves *nonlinear interactions* between the auxiliary source and the thermoacoustic process taking place in the engine.

However, several points remain to be addressed before to draw further conclusions. Notably, several questions are still open concerning the source. Firstly, only one position of the source among the three possibilities has been studied so far; the two other setups will be explored. The same remark is also valid for the microphone driving the feedback loop: only one position among three possibilities has been tested. Secondly, the coupling between the engine and the auxiliary source has been realized empirically, with a quite wide coupling pipe. Other coupling conditions will be tried out, in particular in

order to reduce the increase of the difference temperature caused by the addition of the auxiliary source. Lastly, the presence of the auxiliary source seemingly changes the behavior of the engine in such a way that the optimal load applied at the terminals of the alternator is not the same.

Such projects as the development of thermo-acousto-electric engines are invested in a sustainable development approach. For instance, the collection of waste heat (such as the one produced by a combustion engine) might be interesting to power *low-temperature* thermoacoustic engines. The use of active control, which seems to lower the operating temperature as well as increasing the efficiency, looks promising enough to make relevant the pursuit of this work in that direction. Future works will be devoted to further experimental as well as theoretical studies to clarify the points mentioned above.

References

[1] B. Higgins. cited by W. Nicholson, On the sound produced by a current of hydrogen gas passing through a tube. With a letter from Dr. Higgins, respecting the time of its discovery. *J. Nat. Phil., Chem., and the Arts*, 1:129–131, 1802.

[2] C. Sondhauss. Über die Schallschwingungen der Luft in erhitzten Glasröhren und in gedeckten Pfeifen von ungleicher Weite. *Ann. Phys. (Berlin)*, 155(1):1–34, 1850.

[3] P.L. Rijke. Notiz über eine neue Art, die in einer an beiden Enden offenen Röhre enthaltene Luft in Schwingungen zu versetzen. *Ann. Phys. (Berlin)*, 183(6):339–343, 1859.

[4] Baron J.W.S. Rayleigh. *The theory of sound*, volume 2. Macmillan, 1896.

[5] R.L. Carter, M. White, and A.M. Steele. Private communication of Atomics International Division of North American Aviation. *Inc., September*, 24, 1962.

[6] N. Rott. Thermoacoustics. *Adv. Appl. Mech.*, 20:135–175, 1980.

[7] T. Yazaki, A. Tominaga, and Y. Narahara. Experiments on thermally driven acoustic oscillations of gaseous helium. *J. Low Temp. Phys.*, 41(1-2):45–60, 1980.

[8] J. Wheatley, T. Hofler, G.W. Swift, and A. Migliori. Understanding some simple phenomena in thermoacoustics with applications to acoustical heat engines. *Am. J. Phys*, 53(2):147–162, 1985.

[9] P.H. Ceperley. A pistonless Stirling engine—the traveling wave heat engine. *J. Acoust. Soc. Am.*, 66:1508, 1979.

[10] T. Yazaki, A. Iwata, T. Maekawa, and A. Tominaga. Traveling wave thermoacoustic engine in a looped tube. *Phys. Rev. Lett.*, 81(15):3128–3131, 1998.

[11] S. Backhaus and G.W. Swift. A thermoacoustic Stirling heat engine. *Nature*, 399(6734):335–338, 1999.

[12] S. Backhaus, E. Tward, and M. Petach. Traveling-wave thermoacoustic electric generator. *Appl. Phys. Lett.*, 85(6):1085–1087, 2004.

[13] W.C. Ward and G.W. Swift. Design environment for low-amplitude thermoacoustic engines. *J. Acoust. Soc. Am.*, 95(6):3671–3672, 1994.

[14] W.C. Ward, G.W. Swift, and J.P. Clark. Interactive analysis, design, and teaching for thermoacoustics using DeltaEC. *J. Acoust. Soc. Am.*, 123(5):3546–3546, 2008.

[15] M. Guedra, G. Penelet, P. Lotton, and J.-P. Dalmont. Theoretical prediction of the onset of thermoacoustic instability from the experimental transfer matrix of a thermoacoustic core. *J. Acoust. Soc. Am.*, 130:145, 2011.

[16] A.M. Fusco, W.C. Ward, and G.W. Swift. Two-sensor power measurements in lossy ducts. *J. Acoust. Soc. Am.*, 91:2229, 1992.

[17] S. Backhaus and G.W. Swift. A thermoacoustic-Stirling heat engine: Detailed study. *J. Acoust. Soc. Am.*, 107:3148, 2000.

[18] M.E.H. Tijani and S. Spoelstra. A high performance thermoacoustic engine. *J. Appl. Phys.*, 110(9):093519–093519, 2011.

[19] C. Desjouy, G. Penelet, and P. Lotton. Active control of thermoacoustic amplification in an annular engine. *J. Appl. Phys.*, 108:114904, 2010.

[20] G. Penelet and T. Biwa. Synchronization of a thermoacoustic oscillator by an external sound source. *Am. J. Phys.*, 81:290, 2013.